JOURNAL OF Applied Polymer SCIENCE

Cold-Crystallization Behavior of Poly(L-lactide)/ACR Blend Films Investigated by *In Situ* FTIR Spectroscopy

Ningjing Wu, Honghao Wang, Meichun Ding, Liu Man, Jianming Zhang

Key Laboratory of Rubber-Plastics, Ministry of Education/Shandong Provincial Key Laboratory of Rubber-Plastics, Qingdao University of Science and Technology, Qingdao City 266042, People's Republic of China

Correspondence to: N. Wu (E-mail: ningjing_wu@yahoo.com.cn)

ABSTRACT: The cold crystallization behavior of poly (L-lactide) (PLLA) blend films modified by small amount of acrylic rubber particles (ACR) have been investigated by *in situ* Fourier-transform infrared (FTIR) spectroscopy. During the isothermal cold crystallization, the crystallization rate of PLLA is greatly improved with addition of only 1 wt % ACR. However, for PLLA with 8 wt % ACR, the crystallization rate is slower than that of neat PLLA. The relative crystallinity of PLLA with the addition of 1–5 wt % ACR is obviously higher than that of the neat PLLA. For the PLLA blend film with 3 % ACR, the relative crystallinity reaches a maximum. It was found that the addition of ACR particles below 5% accelerated the cold crystallization nucleation process and made the cold-crystallization rate of PLLA/ACR be quicker than that of neat PLLA. © 2012 Wiley Periodicals, Inc. J. Appl. Polym. Sci. 000: 000–000, 2012

KEYWORDS: PLLA; ACR; cold crystallization; FTIR; blend

Received 27 December 2011; accepted 1 May 2012; published online
DOI: 10.1002/app.37989

INTRODUCTION

Poly(L-lactide) (PLLA) is a biodegradable, biocompatible semi-crystalline polymer that can be synthesized from renewable resources.[1–3] It is a promising biomaterial for biomedical applications such as implant materials, surgical suture, and controlled drug delivery systems. PLLA crystal structure and crystalline behavior have been extensively investigated by many techniques.[4–6] Until now, PLLA crystalline in α, β, γ-conform crystals have been identified, depending on the different preparation conditions. The most common modification, α-form is generally developed from the normal cold, melt, or solution crystallization or low draw ratios.[7] De Sanctis and Kovacs[8] first determined chain conformation of α phase to be a left-handed 10/3 helix, that packs into an orthorhombic unit cell with parameters $a = 1.06$ nm, $b = 1.737$ nm, and $c = 2.88$ nm. The β modification is developed upon mechanical stretching of the more stable α form, or from solution-spinning processes conducted at high temperatures or high hot-draw ratios.[7,9] Hoogsteen et al. suggested an orthorhombic unit cell with $a = 1.031$ nm, $b = 1.821$ nm, and $c = 0.900$ nm, and a chain conformation with left handed 3/1 helices.[7] A third crystal modification of PLLA, γ the form, has been found to develop upon epitaxial crystallization on hexamethylbenzene substrate and has two antiparallel helices packed in an orthorhombic unit cell with $a = 0.995$ nm, $b = 0.625$ nm, and $c = 0.88$ nm.[10] The spherulite growth rate of PLLA is a wide temperature range from 70 to 165°C has been determined. The crystallization rate of PLLA is very high at temperature between 100 and 120°C. Recently, a new limit-disordered modification, designated as α'-form has been proposed for the PLLA samples crystallized below 120°C, different from α order form crystallized at higher temperature (>120°C).[11,12]

PLLA has high modulus and strength comparable to that of many petroleum-based plastics, but its low toughness, low heat deflection temperature, and physical aging restricted its expansion into new application areas. As blending is simple and more economic way compared with copolymer synthesis, much attention has been focused on the blends of PLLA with various materials. Various low molecular weight compounds and oligomers have been investigated as plasticizers for PLLA.[13,14] In general, PLLA blends with low molecular weight compounds can drastically lower the T_g of PLLA, thus create homogeneous and flexible materials. However, the plasticizers have a tendency to migrate to the surface, which would cause material embrittlement. Moreover, the decreased T_g may affect the processing and molding of final products. PLLA has also been blended with some biodegradable polymers such as poly(ε-caprolactone),[15] poly(ethylene glycol),[16] poly(propylene glycol),[17] poly(hydroxyl

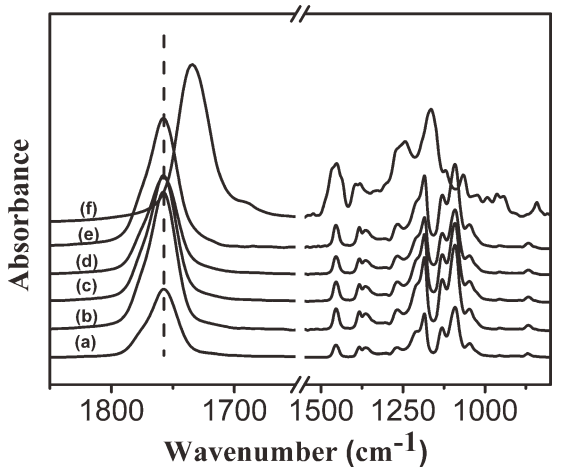

Figure 1. FTIR spectra of PLLA/ACR blend films with various compositions measured at room temperature (a) neat PLLA, (b) PLLA/ACR = 99/1 w/w, (c) PLLA/ACR = 97/3 w/w, (d) PLLA/ACR = 95/5 w/w, (e) PLLA/ACR = 92/8 w/w, and (f) ACR w/w.

butyrate),[18] and other polymers.[19] In general, the toughness of PLLA blend increases, the process ability and tensile strength would be decreased because of their thermodynamically immiscibility and phase segregation.

ACR is the core–shell acrylate elastomer particles, which is used as a very effective impact modifier for polyvinyl chloride (PVC).[20,21] Poly(butyl acrylate) (PBA) rubbery inner core in ACR particles is the dominant toughening material, and the shell phase that consists of poly(methyl methacrylate) (PMMA) could effectively enhance the interfacial adhesion between the core and PVC matrix. For the PVC/ACR toughening system, the impact strength of PVC blend with only 5 wt % increases three times by comparing with neat PVC.[22] It is known that PMMA and PLLA have similar polarity and solubility parameter (δ_{PMMA} = 18.6; δ_{PLLA} = 18.9 ($J^{1/2}$ $cm^{-3/2}$)).[23] ACR in the PLLA could also serve as a modified agent, because PMMA phase at the ACR interphase could decrease the interfacial tension between PLLA matrix and ACR particles. The toughness properties of PLA blend modified by addition of an acrylic modifier were improved. The mechanical measurement results showed that the addition of an acrylic modifier to the PLA significantly lowered the yield stress because of the formation of many void and the relaxation of stress concentration.[24]

Fourier-transform infrared spectroscopy (FTIR) is sensitive to the conformation and local molecular environment of polymers. It has been used as a powerful tool for the analysis and characterization of PLLA due to its distinct IR absorption patterns of amorphous and crystalline components.[11,25] To study the effect of small amount of ACR particles on the cold crystallization behavior of PLLA, the *in situ* FTIR measurement have been made by monitoring the cold crystallization process of PLLA.

EXPERIMENTAL

Materials

PLLA pellets (Natureworks 2002D, M_w = 38 × 10^4 g mol^{-1}, M_w/M_n = 1.59) were purchased from America Nature Works Company. ACR particles (M_w = 30 × 10^4 g mol^{-1}) were supplied by Qingdao University of Science and Technology in China. The average size of ACR particles is about 100 nm, and the thickness of the shell PMMA layer is about 20–30 nm. The PBA/PMMA weight ratio is 70/30 (w/w).

FTIR Spectroscopy Measurement

Infrared spectra were measured by a Bruker Tensor 27 spectrometer equipped with a DTGS detector. The samples were cast on KBr windows from 1% (w/v) PLLA and PLLA blend chloroform solutions, after the majority of the solvent had been evaporated, the thin film was placed under vacuum at 25°C for 48 h to completely remove the residual solvent. Special attention was paid to ensure that the film examined was sufficiently thin to be within the absorption range where Beer-Lambert law was obeyed. IR spectra verified that the film prepared was amorphous. For studying the cold crystallization process of PLLA by *in situ* FTIR spectroscopy, the sample was set on a homemade variable temperature cell, which was placed in the sample compartment of Nicholet spectrometer. The samples was heated at 10°C/min up to 80°C and annealed at 80°C for 2 h. All the IR spectra of the specimen were collected by averaging 16 scans and a resolution of 4 cm^{-1} with 1 min interval during the annealing process.

RESULTS AND DISCUSSION

Cold-Crystallization Behavior of PLLA and PLLA/ACR Investigated by *In Situ* FTIR Measurement

Figure 1 shows FTIR spectra of PLLA/ACR blends with various contents of ACR measured at room temperature in the region of 2000 cm^{-1} to 800 cm^{-1}. For ACR, the band at 1734 cm^{-1} is ascribed to the C=O stretching mode of poly(methyl methacrylate (PMMA) and poly(butyl acrylate) (PBA), the bands at 1243 cm^{-1} and 1164 cm^{-1} are the stretching vibrations of C—O—C groups, and the band at 1381 cm^{-1} is assigned to CH_3 bending vibration. For PLLA/ACR blends, the characteristic bands of ACR from 1500 cm^{-1} to 1000 cm^{-1} are not obvious because of the overlapping and low content of ACR.

Figure 2 shows IR spectra of PLLA cast films used for cold crystallization before and annealing at 80°C for 2 h and the

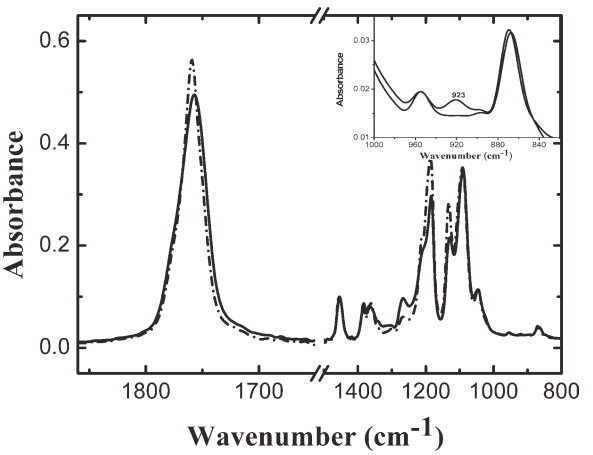

Figure 2. FTIR spectra of the PLLA samples used for cold crystallization before (——) and after annealing at 80°C (- - -) for 120 min.

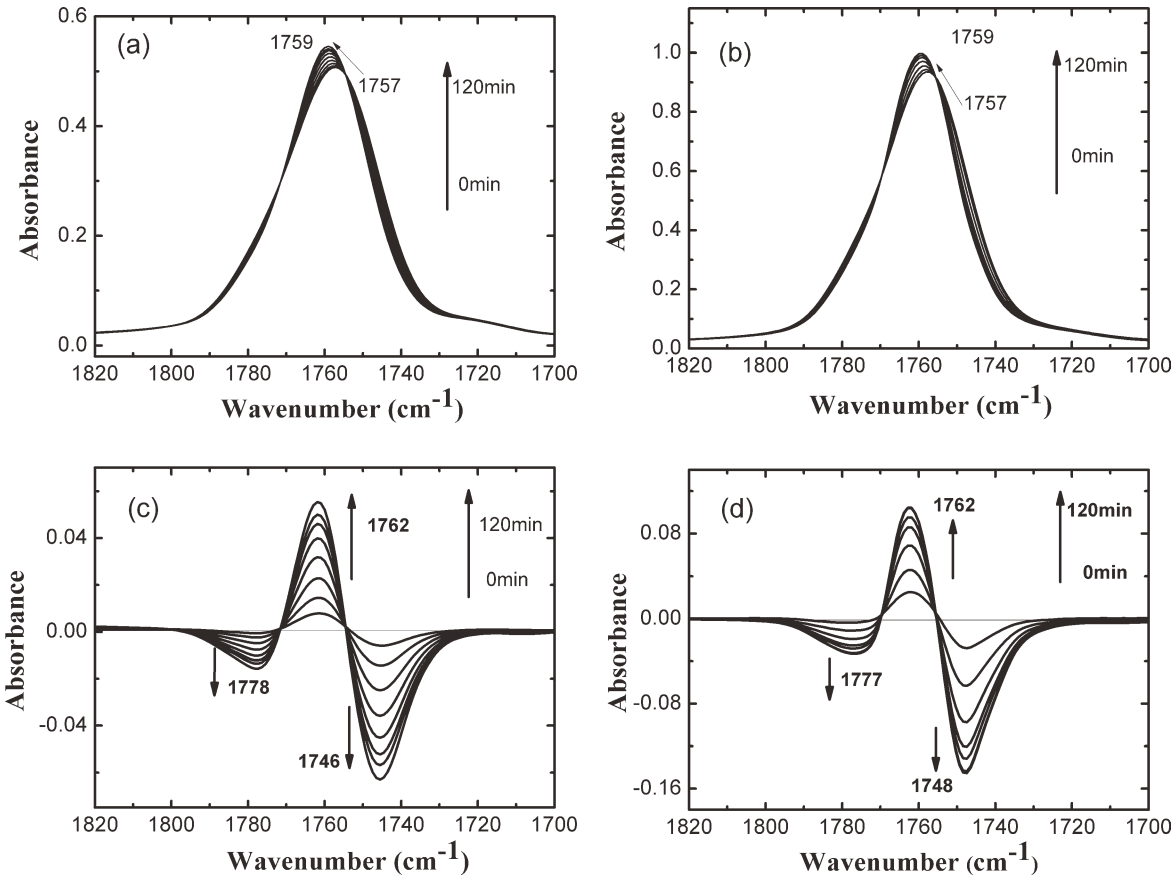

Figure 3. (a and b) Temporal changes of the FTIR spectra in the wave number range of 1820 cm^{-1} to 1700 cm^{-1} during the cold crystallization process of PLLA and PLLA/ACR blend = 97/3 at 80°C. The spectra were arranged with a 10 min interval. (c and d) Difference spectra calculated by subtracting the initial spectrum from the spectra shown in (a and b).

enlarged spectra region in the 1000 cm^{-1} to 820 cm^{-1} is in the set of Figure 2. The IR spectrum of PLLA cast film before annealing shows the complete lack of the band at 921 cm^{-1}, which is assigned to the coupling of C—C backbone stretching with the CH_3 rocking modes and is sensitive to the 10_3 helix chain conformation of PLLA α or α′ crystals.[11] It indicates that the initial state of sample prepared for the cold crystallization is the amorphous.

The spectral evolution in the C=O stretching region during the cold-crystallization process is shown in Figure 2. Because of the dipole–dipole interaction between the C=O bands during the crystallization process of PLLA,[25] it is observed that ν(C=O) spectral region is shifted to a high wave number from 1757 cm^{-1} to 1759 cm^{-1} as shown in Figure 3(a,b). Difference spectra calculated by subtracting the initial spectrum from the rest of spectra in Figure 3(a,b) are displayed in Figure 3(c,d). Obviously, during the crystallization process, the intensity of a positive peak at 1762 cm^{-1} increases gradually with time, whereas the intensity of a negative peak at 1746 cm^{-1} decreases, because 1762 cm^{-1} is the ν(C=O) characteristic band in the crystalline phase and 1746 cm^{-1} is the ν(C=O) characteristic band in the amorphous phase. Compared with Figure 3(c), the variation of peak position of C=O in Figure 3(d) at 1757 cm^{-1} is very similar. In particular, the characteristic band at 1749 cm^{-1} is also not present with the cold crystallization time in above two figures. It means that α′ crystals of PLLA are predominantly formed in the PLLA/ACR blend film at cold crystallization.[26] It can be concluded that ACR has no discernible effect on the crystal structure of PLLA.

From the original spectra of PLLA and PLLA/ACR blend in Figure 4(a,b), the relatively large changes occur in the C—O—C stretching region from 1500 cm^{-1} to 1000 cm^{-1}. To emphasize the spectral changes and to relate the intensity changes of these peaks to the crystallization kinetics, a series of difference spectra are calculated by subtracting the initial spectrum from the semicrystalline state spectra displayed in Figure 4(c,d). The new positive peaks at 1193 cm^{-1}, 1135 cm^{-1}, and 1108 cm^{-1} increase with the annealing time, which are assigned to the vibrational modes involving the C—O—C stretching with the planar trans conformational state of ester group in the crystalline phase of PLLA, whereas the intensity of a negative peak at 1267 cm^{-1} decreases, because the 1267 cm^{-1} band is assigned to the combination of ν(CH) and ν(C—O—C) in the amorphous phase. The band at 1212 cm^{-1} shifts to 1215 cm^{-1}, because the C—O—C backbone is prone to form the ordered helix conformation of polymer chain.[26] Compared with Figure 4(c), the variation trend of each peak position in Figure 4(d) is similar, and the intensity change in Figure 4(d) for PLLA/ACR blend is stronger than that of neat PLLA in Figure 4(c).

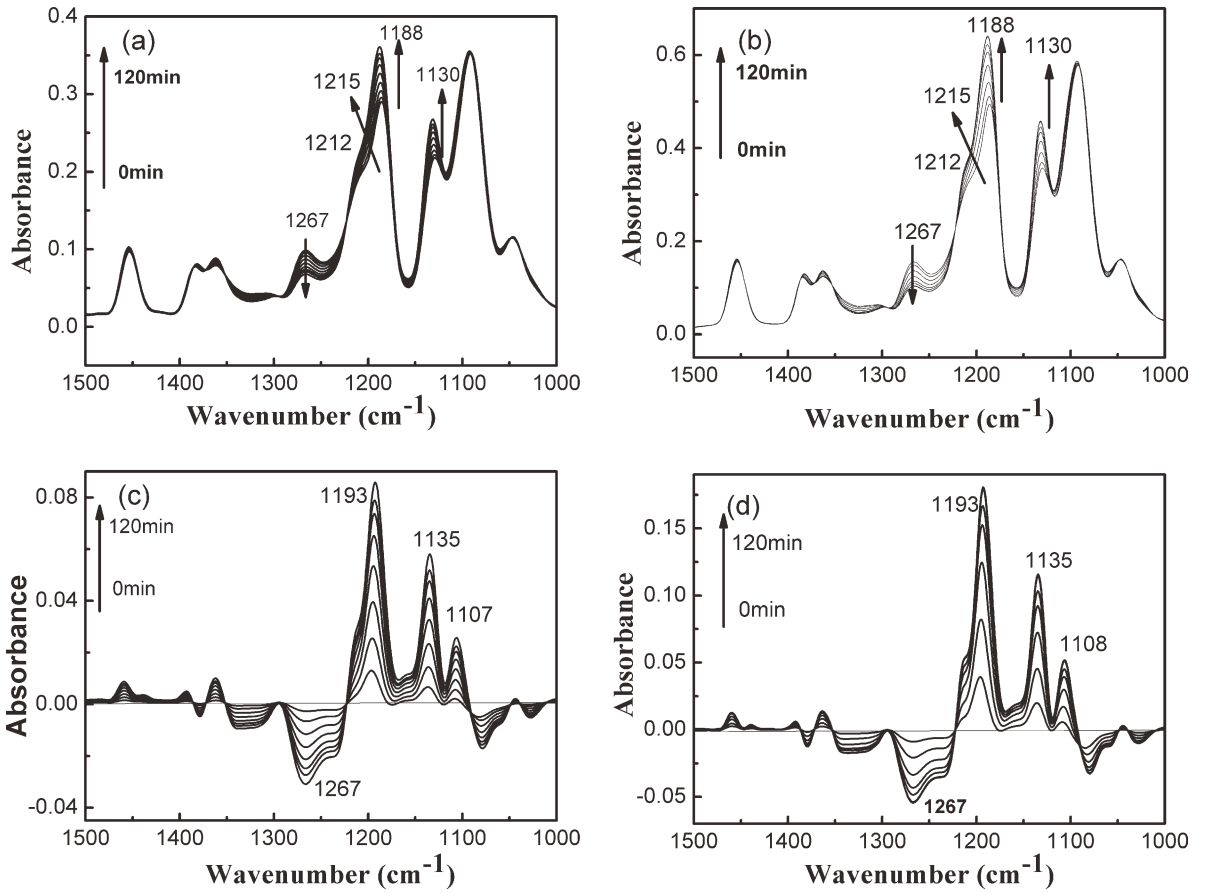

Figure 4. (a and b) Temporal changes of the FTIR spectra in the wave number range of 1500 cm^{-1} to 1000 cm^{-1} during the cold crystallization process of PLLA and PLLA/ACR blend = 97/3 at 80°C. The spectra were arranged with a 10 min interval. (c and d) Difference spectra calculated by subtracting the initial spectrum from the spectra shown in (a and b).

Isothermal Crystallization Kinetics of PLLA/ACR Blend Samples

To demonstrate the influence of ACR content on the cold crystallization rate of PLLA, the isothermal crystallization kinetics of PLLA and PLLA/ACR blends are systematically studied. The Avrami equation is often used to analyze the isothermal crystallization process of polymer. When IR data in difference spectra are used, Avrami's equation was used as follows[27,28]:

$$\frac{A_t - A_\infty}{A_0 - A_\infty} = \exp(-kt^n)$$

Here A_t is the peak intensity at the crystallization time t, A_0 and A_8 are, respectively, the initial and final peak intensities during isothermal crystallization, k is the crystallization rate constant dependent on the nucleation and growth rates, t is the time of the crystallization, and n is the Avrami exponent, which is related to the nature of nucleation and the geometry of the growing crystals.

In cold crystallization process, the crystallization characteristic absorption peaks at 1130, 1188, 1760 cm^{-1} increase with crystallization time. Meanwhile, the amorphous characteristic absorption peak at 1267 cm^{-1} decreases with the crystallization time. The normalized peak heights of the crystalline sensitive band at 1130 cm^{-1} and amorphous sensitive band at 1267 cm^{-1} of PLLA and PLLA/ACR are plotted as a function of crystallization time at 80°C in Figure 5, respectively.

From Figure 5, it is found that the addition of ACR in the PLLA matrix has obvious influence on the cold crystallization rate of PLLA. For PLLA with the addition of 1–5 wt % ACR, the crystallization rate is obviously higher than that of the neat PLLA. In particular, the crystallization rate of PLLA is greatly improved with addition of only 1 wt % ACR. However, for PLLA with 8 wt % ACR, the crystallization rate is slower than that of neat PLLA.

For further comparison of the crystallinity of PLLA blend films with the different compositions of ACR, we choose the crystalline characteristic peak (1130 cm^{-1} or 1760 cm^{-1}) and amorphous peak (1267 cm^{-1}), the relative crystallinity of PLLA is represented by the ratio value of the intensity at 1267 cm^{-1} divided by that of 1130 cm^{-1} or 1760 cm^{-1}.[25,26] The dependence of the relative crystallinity on the crystallization time for PLLA and PLLA/ACR blends are shown in Figure 6. From Figure 6(a), we can see that the relative crystallinity of PLLA films with below 5 wt % ACR content is higher than that of neat PLLA. At the beginning, the crystallinity rate of PLLA with 1 wt % ACR is obviously higher than that of neat PLLA, so the degree

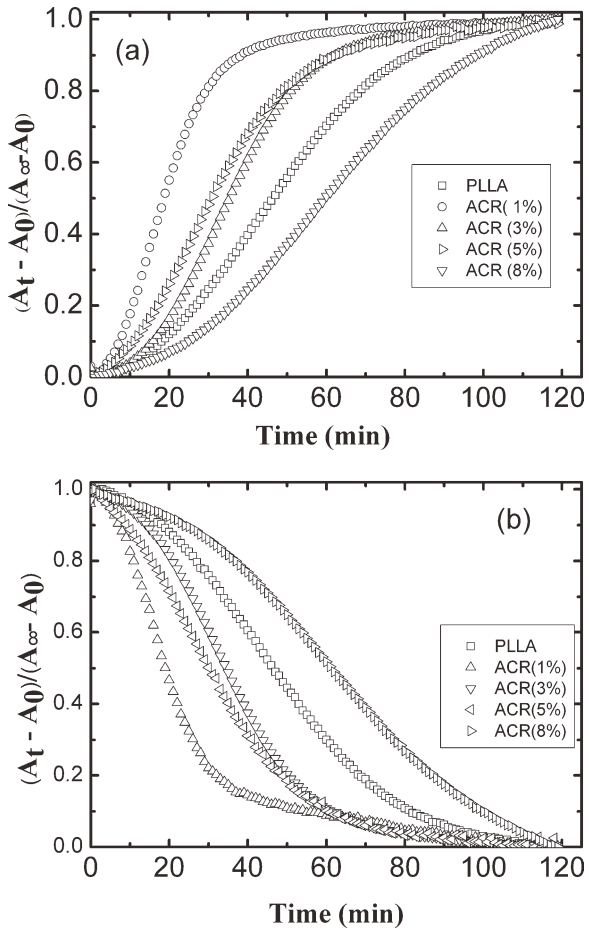

Figure 5. Normalized peak heights of the crystalline sensitive bands of PLLA and PLLA/ACR blends as a function of crystallization time at 80°C calculated from the difference spectra shown in Figure 4(a) at 1130 cm^{-1} (b) 1267 cm^{-1}.

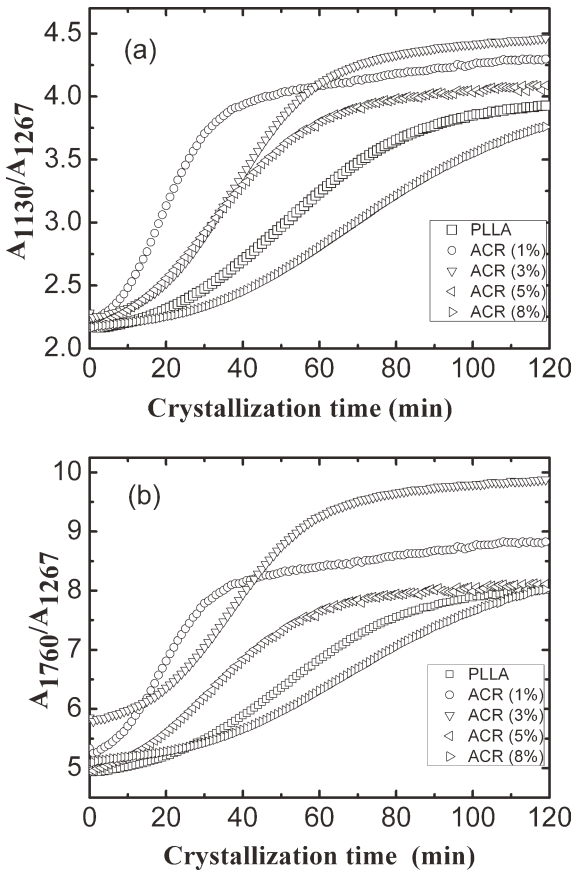

Figure 6. Temporal changes of relative crystallization degree dependence on the crystallization time for PLLA and PLLA/ACR blends (a) calculated from the intensity at 1267 cm^{-1} were divided by that at 1130 cm^{-1} (b) calculated from the intensity at 1267 cm^{-1} were divided by the intensity at 1760 cm^{-1}.

of relative crystallinity of PLLA sharply increases, and then levels off after about 60 min. With the increasing of ACR content, the increment trend of the degree of relative crystallinity of PLLA with time slows down. For the PLLA blend film with 3% ACR, the relative crystallinity reaches a maximum at 120 min. However, with the further increase of ACR, for the content of ACR is 8 wt %, the relative crystallinity is lower than that of neat PLLA at 120 min as shown in Figure 6(a), but the crystallinity of PLLA blend sample could further increase with crystalline time. Finally, it may exceed the corresponding relative crystallinity degree of neat PLLA as shown in Figure 6(b).

Equation 1 can also be expressed in the following form.

$$\ln\left[-\ln\left(\frac{A_t - A_\infty}{A_0 - A_\infty}\right)\right] = \ln k + n \ln t$$

Accordingly, the Avrami parameters n and k can be obtained from the slope and the intercept, respectively, by plotting the first term versus ln t. Using the peak height of the band at 1130 cm^{-1} during the isothermal cold crystallization of PLLA at 80°C, the plot of $\ln[-\ln((A_t - A_\infty)/(A_0 - A_\infty))]$ versus ln t of PLLA blend with 3 wt % ACR content is plotted in Figure 7. The curve exhibits a good linear relationship, which suggests that the isothermal crystallization kinetics of PLLA/ACR blend film is in good agreement with the Avrami equation. The curve obviously deviates from the linear in crystallization stage, which

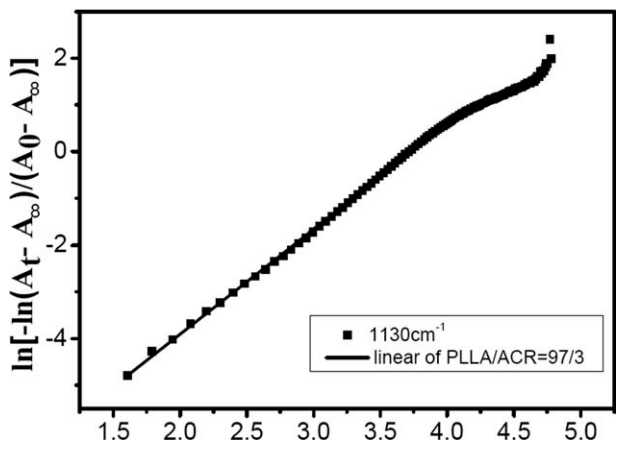

Figure 7. The plot of Avrami equation for the analysis of isothermal cold crystallization of PLLA/ACR blend film at 80°C for 120 min.

Table I. Avrami Parameters Derived from the Analysis of Isothermal Cold Crystallization of PLLA and PLLA/ACR Blend Films at 80°C Using the Normalized Peak Height at 1130 cm^{-1}

Composition PLLA/ACR	Parameters			
	n	Ln k	$T_{1/2}$ (min)	k (min^{-n} $\times$ 10^4)
100/0	2.0	−7.99	45.3	3.4
99/1	2.0	−6.77	24.5	11.5
97/3	2.0	−7.50	35.4	5.5
95/5	2.0	−7.22	30.8	7.3
92/8	2.0	−8.45	56.9	2.1

was thought to be due to the secondary crystallization that is caused by the spherulite impingement in the later stage.

The parameters of crystallization kinetics calculated according to same band shown in Figure 7 are listed in Table I. For isothermal cold crystallization of PLLA at 80°C, the average value of the Avrami exponent is 2. It is very close to the value reported from previous literature.[22] This is suggested that the crystallization of PLLA film started from heterogeneous nucleation and the primary crystallization stage is a two-dimensional, circular, diffusion-controlled growth of nucleation. For PLLA with several percent ACR, the value Avrami exponent n is about 2, it can be thought that the nucleation mode of PLLA with adding small amount of ACR is not changed, and it maintains two-dimensional nucleation growth.

Crystallization half-life ($t_{1/2}$) is defined as the time at which 50% of the normalized crystallinity is reached; $t_{1/2}$ can be expressed as follows:

$$t_{1/2} = \left(\frac{\ln 2}{k}\right)^{1/n}$$

Table I shows the crystallization half-time, $t_{1/2}$ and crystallization rate constant, k. For PLLA with the addition of 1 wt % ACR, $t_{1/2}$ is only 24.5 min, it is obviously smaller than that of neat PLLA ($t_{1/2}$ = 44.7 min). K is also represents the crystallization rate. For PLLA film with the addition of 1 wt % is 11.5 $\times$ 10^{-4} min^{-2}, which is larger than that of neat of PLLA (3.4 $\times$ 10^{-4} min^{-2}). It means the crystallization rate is increased with low content of ACR particles, the data listed in Table I demonstrated that the incorporation of less than 5 wt % ACR increases the crystallization rate of PLLA.

In fact, the crystallization kinetics of semicrystalline blend is related to the nucleating effect induced by the addition of ACR particles. As is well known, when the heterogeneous nucleating agent is added to polymer, an increase in the overall crystallization rate occurs with a reduction of the nucleation induction period and an increase in the number of primary nucleation sites. The addition of ACR enhanced the formation of PLLA crystal nucleus. With the addition of ACR, the nucleus density of crystallites was largely increased, so the crystallization rate of PLLA with the small amount of ACR is higher than that of neat PLLA. However, with the further increasing of ACR content, for example, $t_{1/2}$ of PLLA with the addition 8 wt % is 56.1 min, which is larger than that of neat PLLA. It is because more ACR particles in the PLLA matrix hinder crystal growth process of PLLA. That is consistent with the result from Figure 6.

CONCLUSIONS

In this article, PLLA has been modified with small amount of ACR particles. The *in situ* FTIR measurement results indicate that small amount of ACR will accelerate the cold crystallization rate of PLLA because small amount of ACR are effective nucleating agents during the cold crystallization of PLLA. In particular, the crystallinity rate of PLLA is greatly improved with addition of only 1 wt % ACR; its crystallinity half-time is only nearly half of that of neat PLLA. However, with the increase of ACR content, the crystallization rate of PLLA declines, because more ACR particles hinder the cold crystallization growth process of PLLA. The relative crystallinity degree of PLLA with the addition of 1–5 wt % ACR is obviously higher than that of the neat PLLA. For the PLLA blend film with 3% ACR, the relative crystallinity degree reaches a maximum. With the increasing of ACR content, the increment trend of the degree of relative crystallinity of PLLA with time slows down.

The cold crystallization kinetics results indicate that the crystallization of PLLA film with several percent of ACR particles started from heterogeneous nucleation and the nucleation mode still remains a two-dimensional, circular, diffusion-controlled growth of nucleation.

The authors are grateful for the financial supports from Natural Science Foundation of China (21104038, 21074063), Shandong Province Science Foundation for Distinguished Young Scholars (JQ200905), Taishan Mountain Scholar Constructive Engineering Foundation (TS20081120), and Doctoral Foundation of Shandong Province (2010BSE08010).

REFERENCES

1. Gross, R. A.; Kalra, B. *Science* **2002,** *297*, 803.
2. Ikada, Y.; Tsuji, H. *Macromol. Rapid Commun.* **2000,** *21*, 117.
3. Cai, H.; Dave, V.; Gross, R. A.; Mc Cathy, S. P. *J. Polym. Sci. Part B: Polym. Phys.* **1996,** *34*, 2701.
4. Puiggali, J.; Ikada, Y.; Tsuji, H.; Cartier, L.; Okihara, T.; Lotz, B. *Polymer* **2000,** *41*, 8921.
5. Sasaki, S.; Asakura, T. *Macromolecules* **2003,** *36*, 8385.
6. Kikkawa, Y.; Abe, H.; Iwata, T.; Inoue, Y.; Doi, Y. *Biomacromolecules* **2002,** *3*, 350.
7. Hoogsteen, W.; Postema, A. R.; Pennings, A. J.; Ten Brinke, G.; Zugenmaier, P. *Macromolecules* **1990,** *23*, 634.
8. De Sanctis, P.; Kovacs, A. *Biopolymers* **1968**, *6*, 299.
9. Puiggali, J.; Ikada, Y.; Tsuji, H.; Cartier, L.; Okihara, T.; Lotz, B. *Polymer* **2000,** *41*, 8921.
10. Cartier, L., Okihara, T.; Ikada, Y.; Tsuji, H.; Puiggali, J.; Lotz, B. *Polymer* **2000,** *41*, 8909.

11. Zhang, J. M.; Duan, Y. X.; Sato, H.; Tsuji, H.; Noda, I.; Yan, S.; Ozaki, Y. *Macromolecules* **2005,** *38*, 8012.
12. Zhang, J. M.; Tashiro, K.; Tsuji, H.; Domb, A. J. *Macromolecules* **2008,** *41*, 1352.
13. Ljungberg, N.; Wesslen, B. *Biomacromolecules* **2005,** *6*, 1789.
14. Martin, O.; Averous, L. *Polymer* **2001,** *42*, 6209.
15. Na, Y. H.; He, Y.; Shuai, X. T.; Kikkawa, Y.; Inoue, Y. *Biomacromolecules* **2002,** *3*, 1179.
16. Kulinski, Z.; Piorkowska, E. *Polymer* **2005,** *46*, 10290.
17. Kulinski, Z.; Piorkowska, E.; Gadzinowska, K.; Stasiak, M. *Biomacromolecules* **2006,** *7*, 2128.
18. Focarete, M. L.; Scanodola, M.; Dobrzynski, P.; Kowalczuk, M. *Macromolecules* **2002,** *35*, 8472.
19. Wang, H.; Sun, X. Z.; Seib, P. *J. Appl. Polym. Sci.* **2001,** *82*, 1761.
20. Hu, Y.; Sato, H.; Zhang, J. M.; Noda, I.; Ozaki, Y. *Polymer* **2008,** *49*, 4204.
21. Yuan, J. F.; Pan, M. W.; Wang, X. M.; Zhang, L. C. *Polym. Eng. Sci.* **2007,** *47*, 996.
22. Yu, J. Y.; Feng, P. C.; Zhang, H. L. *Polym. Eng. Sci.* **2010,** *50*, 295.
23. Wu, P. X.; Zhang, L. C. Polymer Blends Modification; Light Industry Press in China: Beijing, **2004;** pp 37–38.
24. Masakazu, I.; Satomi, A.; Masaru, I. *J. Appl. Polym. Sci.* **2010**, *115*, 1454.
25. Zhang, J. M.; Tsuji, H.; Noda, I.; Ozaki, Y. *Macromolecules* **2004,** *37*, 6433.
26. Zhang, J. M.; Tsuji, H.; Noda, I.; Ozaki, Y. *J. Phys. Chem. B* **2004,** *108*, 11514.
27. Avrami, M. *J. Chem. Phys.* **1939,** *7*, 1103.
28. Avrami, M. *J. Chem. Phys.* **1940,** *8*, 212.